

Controllable Cleavage of C–N Bond-Based Fluorescent and Photoacoustic Dual-Modal Probes for the Detection of H₂S in Living Mice

Jie Zhang,¹ Guohua Wen,¹ Wanhe Wang, Ke Cheng, Qiang Guo, Shuang Tian, Chao Liu, Hanrong Hu, Yachao Zhang, Huatang Zhang, Lidai Wang,* and Hongyan Sun*

Cite This: *ACS Appl. Bio Mater.* 2021, 4, 2020–2025

Read Online

ACCESS |

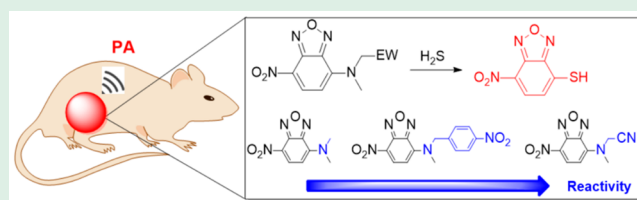
Metrics & More

Article Recommendations

Supporting Information

ABSTRACT: Hydrogen sulfide (H₂S) has been recognized to influence a wide range of physiological and pathological processes. Its underlying molecular events, however, are still poorly understood. An activatable H₂S probe for photoacoustic (PA) imaging is desirable to further explore the role of H₂S in vivo. Nevertheless, only a few activatable PA probes for H₂S detection have been reported. In particular, examples of dual-modal H₂S probes with the combined advantages of fluorescence (high sensitivity and resolution) and PA imaging (deep penetration) are very rare. Herein the controllable cleavage of the C–N bond in nitrobenzoxadiazole (NBD) amine derivatives by H₂S is presented for the first time. The cleavage reactivity was found to be accelerated by the introduction of an electron-withdrawing group. Through this strategy, a series of fluorescent and PA dual-modal probes (1–3) were developed for H₂S detection. Among them, probe 3 shows a high fluorescence on–off response rate ($k_2 = 4.04 \text{ M}^{-1} \text{ s}^{-1}$) and excellent selectivity for H₂S over other biothiols. Moreover, probe 3 can also work as an activatable PA H₂S probe because of the significant shift of its absorption peak from 468 to 532 nm in the H₂S reaction. Importantly, probe 3 demonstrates its capability for fluorescence and PA imaging of H₂S in living cells and mice. These results indicate that the controllable cleavage of the C–N bond can serve as an efficient strategy for designing fluorescent and PA dual-modal H₂S probes.

KEYWORDS: controllable cleavage, fluorescence, photoacoustic, hydrogen sulfide probe, living mice



INTRODUCTION

Hydrogen sulfide (H₂S) has been identified as the third gas transmitter, after nitric oxide and carbon monoxide.^{1–3} Accumulating studies show that H₂S is associated with a wide range of physiological and pathological processes such as regulation in the central nervous, cardiovascular, respiratory, and gastrointestinal systems.^{4,5} Abnormal H₂S levels have been implicated in many diseases, including Alzheimer's disease,⁶ Huntington's disease,⁷ Parkinson's disease,⁸ Down's syndrome,⁹ and cancers.¹⁰ Therefore, sensitive molecular probes for in vivo imaging of H₂S are valuable for exploring the biology of H₂S and diagnosing H₂S-related diseases.

Because of its noninvasive property, fluorescence sensing and imaging of H₂S has emerged as a valuable method for detecting H₂S in biological samples.^{11–17} However, because of strong optical scattering in biological tissue, fluorescence imaging of H₂S suffers from low imaging depth. As an emerging bioimaging technique, photoacoustic (PA) imaging combines diffusive optical excitation and focused ultrasound detection, offering high contrast in deep tissue.^{18–20} However, the sensitivity and the resolution of PA imaging is not high enough compared with fluorescence-based methods. Therefore, it is highly desirable to integrate fluorescence and PA

imaging to achieve deep tissue penetration and high spatial resolution for detecting H₂S in vivo. Although many chemical reactions have been applied in the development of H₂S probes for fluorescent imaging,^{13–17} very few reaction-based H₂S probes have been successfully developed for PA imaging.^{21–26} The reported reaction-based H₂S PA probes mainly utilize the reduction reaction of azide,²¹ nucleophilic substitution (e.g., thiolysis of dinitrophenyl ether),^{22–25} and copper precipitation.²⁶ Most of these probes are monomodal probes that show only a PA signal change toward H₂S. Very recently, He et al.²⁴ and Wu et al.²⁵ both reported elegant works on developing optical/photoacoustic probes to detect H₂S successfully in mice. Nevertheless, fluorescent and PA dual-modal probes are still quite rare. Therefore, the development of new fluorescent and PA dual-modal probes for sensitive and selective detection of H₂S is still highly desired.

Special Issue: Biospecies Sensors

Received: April 14, 2020

Accepted: May 29, 2020

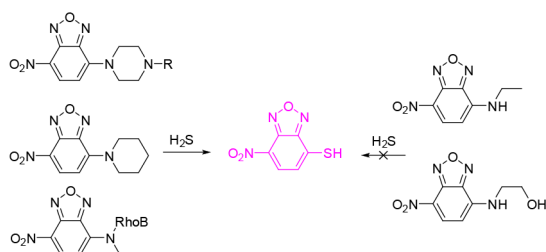
Published: June 11, 2020



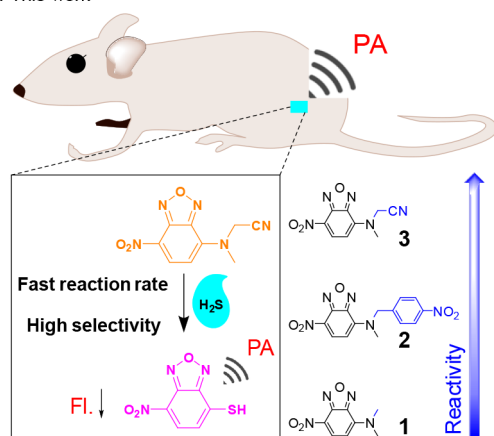
It has been reported that nitrobenzoxadiazole (NBD) amines can undergo H₂S-specific thiolytic cleavage of the C–N bond.²⁷ A number of fluorescent probes have been developed using this strategy.^{28–33} The approach, however, is limited only to piperazinyl- and piperidyl-based NBD probes and a rhodamine B–NBD conjugate (Scheme 1A).^{34–36} In this

Scheme 1. (A) Previously Reported NBD-Amine-Based H₂S Fluorescent Probes; (B) Modular Design of the Fluorescent and PA Dual-Modal H₂S Probes in This Work

A. Previous work on H₂S fluorescent probes



B. This work



study, we reasoned that the cleavage of the C–N bond of the NBD-amine by H₂S can be finely tuned by introducing different electron-withdrawing groups. By comparison of the reactivity of three modularly designed probes (Scheme 1), the cleavage reactivity was found to be accelerated by the presence of an electron-withdrawing group in the amine linkage. On the basis of this reaction, the effective dual-modal probe 3 to detect H₂S with both fluorescence and PA readout was successfully developed (Scheme 1). Upon reaction with H₂S, 2-(methylamino)acetonitrile is cleaved, and probe 3 turns into NBD-SH, resulting in a bathochromic shift and fluorescence signal decrease. On the other hand, the PA signal is significantly enhanced because of the strong absorption of NBD-SH. As a result, probe 3 exhibits both fluorescence quenching and PA signal enhancement in H₂S detection.

RESULTS AND DISCUSSION

One approach to design H₂S probes utilized the substitution reaction of a piperazine/piperidine or rhodamine B moiety on NBD by H₂S (Scheme 1A). The reaction is very specific toward H₂S and inert toward other interfering species such as thiols. Nevertheless, it was reported that when the piperazine/piperidine moiety was changed to other groups such as ethylamino or ethanolamino, the reactivity of the probe with H₂S significantly decreased (Scheme 1A). In this study, we

hypothesized that the introduction of an asymmetrically substituted amine group may allow one to adjust the reaction rate between NBD-based probes and H₂S. By the introduction of an electron-withdrawing group, the leaving group ability of the amine group would be enhanced,^{37,38} resulting in increased cleavage reactivity of the C–N bond by H₂S. Therefore, the reaction rate of the probes with H₂S could be tuned in a controlled manner. We designed a total of three probes in which the electron-withdrawing effect of the amine moiety became stronger from probe 1 to probe 3 (Scheme 1). Probes 1–3 were synthesized through the reaction of NBD-Cl with the corresponding amines containing a methyl group or different electron-withdrawing groups based on the classical S_N2 substitution reaction (Scheme S1). The chemical structures of probes 1–3 were fully characterized by ¹H ¹³C NMR spectroscopy and mass spectrometry (see the Supporting Information).

With the probes in hand, the absorption and fluorescence responses of probes 1–3 toward H₂S were first examined. Probes 1–3 were incubated with H₂S in PB buffer (20 mM with 10% DMSO), and the absorption and fluorescence spectra were recorded accordingly. The results showed that before the reaction, probes 1–3 displayed absorption peaks at ~480 nm, which is the characteristic absorption of NBD-amines.³⁵ After the reaction, the absorption peak was red-shifted because NBD-SH was produced from the cleavage of the C–N bond of the NBD-amine (Figures 1a, S1, and S2). Moreover, the color of the probe solutions with the addition of H₂S changed from yellow to purple (insets of Figures 1a, S1, and S2), showing its potential in the visual detection of H₂S. Meanwhile, the fluorescence signal significantly decreased after probes 1–3 reacted with H₂S, indicating the generation of NBD-SH through the cleavage reaction (Figures S3–S5). To further corroborate this conclusion, HPLC (Figure S6) and mass spectrometry analyses were conducted. The mass spectra unambiguously identified the cleavage product NBD-SH obtained from probes 1–3 upon the addition of H₂S (Figure S7).

To gain insights into the electron-withdrawing effect on the cleavage of the C–N bond, the reaction kinetics of probes 1–3 toward H₂S was investigated. As shown in Figure 1b, the time-dependent fluorescence signals of probes 1–3 at their corresponding maximum emission peaks were recorded. By fitting the fluorescence intensity data to a single-exponential decay function of time, the pseudo-first-order rate constants *k*_{obs} were determined to be 0.009, 0.038, and 0.24 min^{−1} for probes 1, 2, and 3, respectively. Moreover, the reaction rate constants *k*₂ were calculated to be 0.15, 0.63, and 4.04 M^{−1} s^{−1} for probes 1, 2, and 3, respectively (Figure 1b inset). These results demonstrated that the reaction rate was positively correlated with the electron-withdrawing effect, indicating that the rate of cleavage of the C–N bond in the probe can be controlled by introducing different electron-withdrawing groups. Taken together, the results showed that probe 3 was the most reactive, and it emerged as a promising candidate for further experiments.

A titration experiment on probe 3 with various concentrations of H₂S was then performed. The results showed an excellent linear relationship (*R*² = 0.995) between the fluorescence emission at 530 nm and the concentration of H₂S (1–30 μM) (Figure 1c). The detection limit was calculated to be 0.82 μM based on the 3σ/*k* method. Developing highly selective probes that exhibit a distinctive

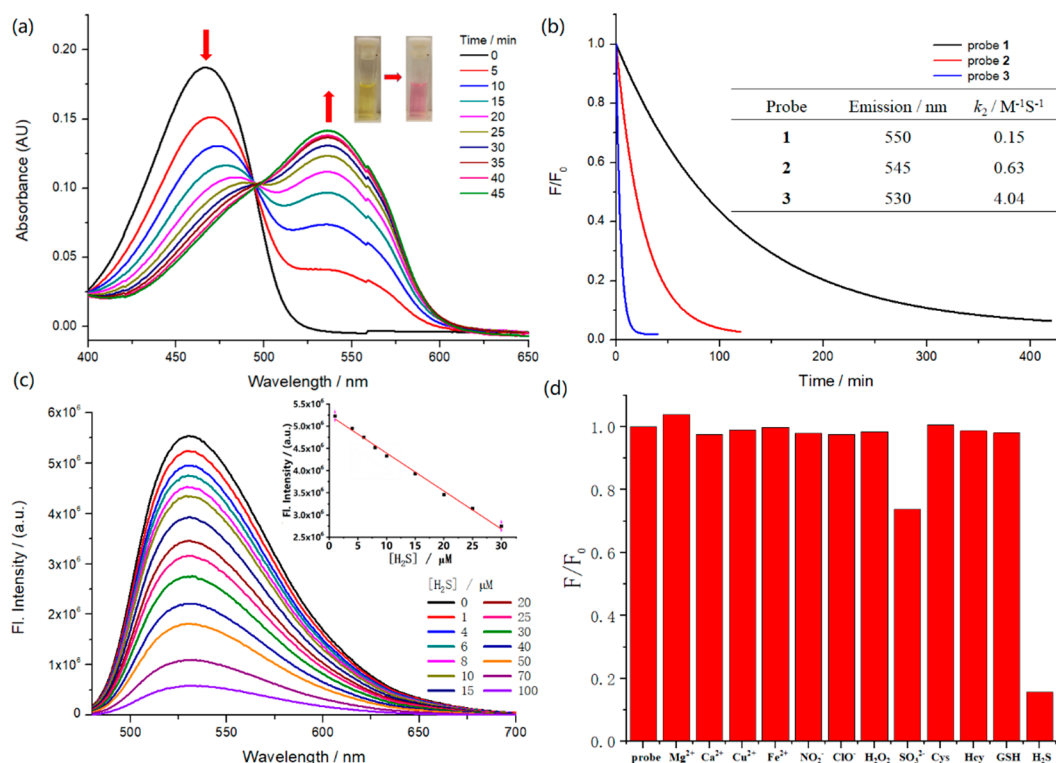


Figure 1. (a) Time-dependent UV–vis spectra of 20 μM probe 3 incubated with 200 μM H₂S in PB buffer (20 mM, pH 7.4, containing 10% DMSO). (b) Kinetic test of the probes with H₂S. The probes (5 μM) were reacted with 1 mM H₂S at room temperature in PB buffer (20 mM, pH 7.4, 10% DMSO). Inset: summary of the emission wavelengths and reaction rate constants (k_2) of the probes. (c) Fluorescence spectra of probe 3 (5 μM) incubated with different concentrations of H₂S. Inset: plot of the fluorescence intensity at 530 nm vs H₂S concentration. (d) Fluorescence intensity ratios of probe 3 (5 μM) at 530 nm in PB buffer (20 mM, pH 7.4, 10% DMSO) in the presence of various species Mg²⁺, Ca²⁺, Cu²⁺, Fe²⁺, NO₂⁻, ClO⁻, H₂O₂, SO₃²⁻, Cys, Hcy, H₂S (200 μM), GSH (1 mM). All of the reaction mixtures were incubated at room temperature for 1 h. λ_{ex} = 465 nm.

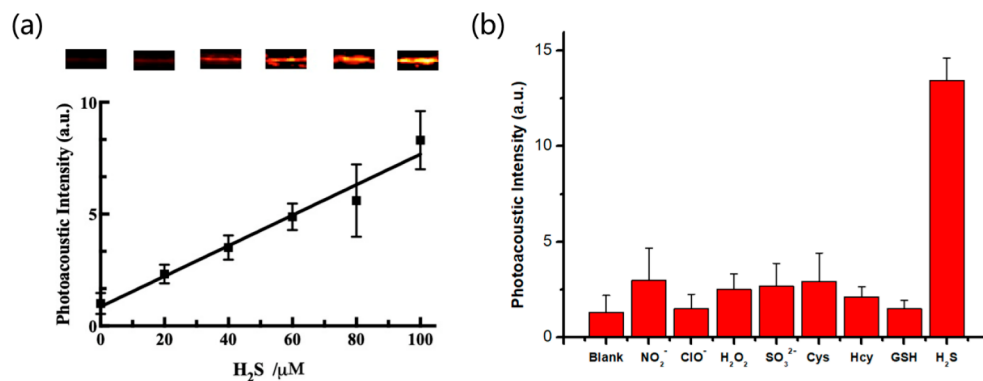


Figure 2. (a) Linear plot of the PA intensities (PA₅₃₂) of probe 3 (20 μM) at different concentrations of H₂S. The detection limit was calculated on the basis of $3\sigma/k$ values, where σ is the standard deviation of three blank measurements and k is the slope of the curve. (b) PA intensity (PA₅₃₂) of probe 3 (20 μM) treated with various biomolecules (GSH, 1 mM; others, 200 μM).

response to H₂S over other biothiols is a major challenge for H₂S detection. To confirm the selectivity of this controllable cleavage of C–N bonds by H₂S, probe 3 was incubated with different metal ions, reactive nitrogen species, reactive oxygen species, or reactive sulfur species. As depicted in Figure 1d, only H₂S showed significant fluorescence quenching. As evidenced by these results, the controllable cleavage of C–N bonds is highly sensitive and selective to H₂S without any distinct interference from most species, except for limited interference from SO₃²⁻. This is consistent with the reported literature.^{27,30,31}

Upon interaction with H₂S, probe 3 was quenched and showed a significantly red-shifted absorption peak at 532 nm. Moreover, the reaction product NBD-SH possessed a large extinction coefficient ($19\,000 \pm 600 \text{ M}^{-1} \text{ cm}^{-1}$), ensuring effective PA detection both in vitro and in vivo.³⁹ Furthermore, probe 3 displayed a high reaction rate and excellent selectivity. We therefore expected that probe 3 could serve as an efficient H₂S probe for PA imaging. We first tested the PA response of probe 3 at different concentrations of H₂S. As expected, strong PA signals were detected when the reaction mixture was excited with a 532 nm laser pulse. A good linear relationship was established between the PA amplitude and the H₂S

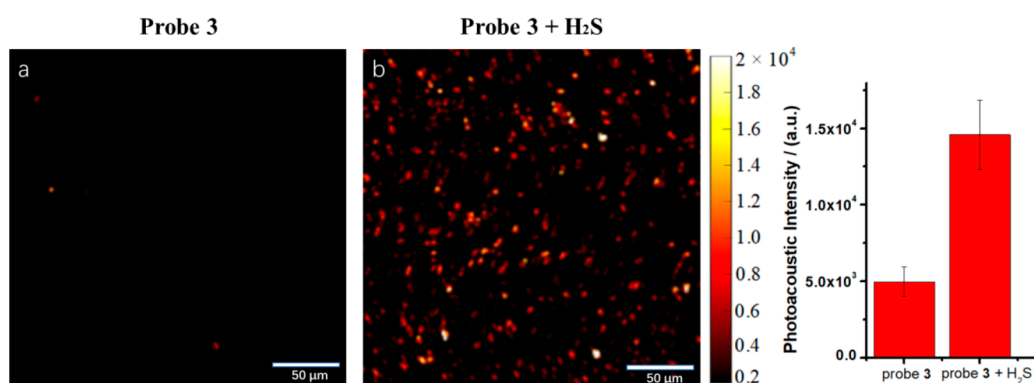


Figure 3. PA imaging of H₂S in HeLa cells. (a) The cells were incubated with 50 μM probe 3 only. (b) The cells were pretreated with 50 μM probe 3 for 30 min and then incubated with H₂S (500 μM) for another 40 min. $\lambda_{\text{ex}} = 532$ nm; pulse energy = 100 nJ. Scale bars: 50 μm.

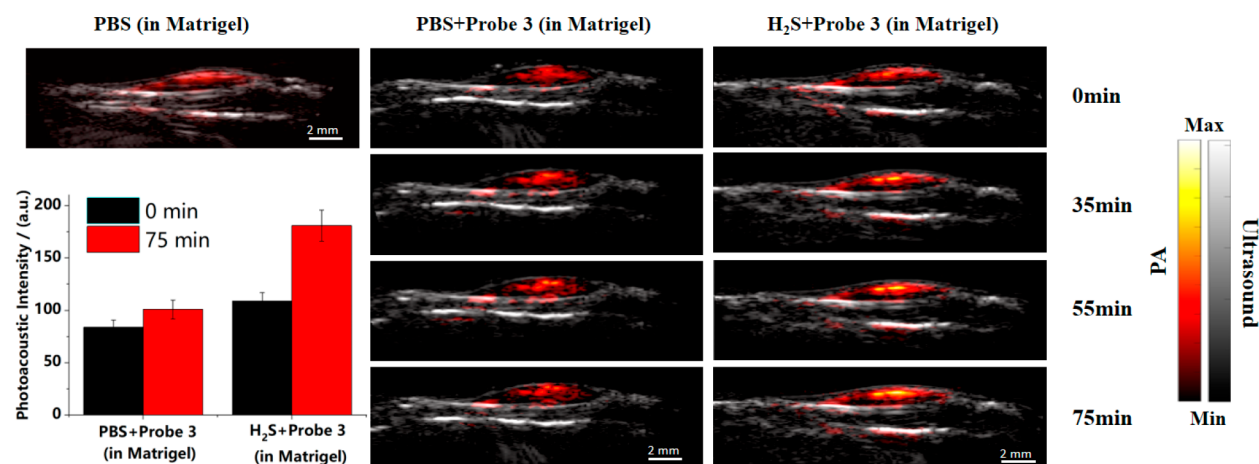


Figure 4. Time-dependent PA imaging experiments with living mice: (left) Matrigel mixed with PBS; (middle) Matrigel mixed with PBS (150 μL) + probe 3; (right) Matrigel mixed with H₂S in PBS (150 μL, final concentration 30 mM) + probe 3. Probe 3 (50 μL, 100 μM) was injected subcutaneously into a leg of each mouse after solidification of the gel. $\lambda_{\text{ex}} = 532$ nm; fluence = 1.5 mJ/cm².

concentration from 0 to 100 μM ($R^2 = 0.987$) (Figure 2a). The detection limit of H₂S was 3.5 μM according to the $3\sigma/k$ method. Furthermore, probe 3 also exhibited excellent PA selectivity toward H₂S over a range of potential interfering species. Upon excitation at 532 nm, the presence of H₂S generated strong PA signals, while only negligible signals were observed in the presence of reactive oxygen species, reactive nitrogen species, or reactive sulfur species under the same excitation (Figure 2b). These results together demonstrated that probe 3 is a highly sensitive and selective PA probe for H₂S detection.

To investigate the biological applicability of probe 3, both fluorescence and PA imaging of H₂S in living cells were carried out. Before imaging, the cytotoxicity of probe 3 was evaluated using the CCK-8 assay with HeLa cells (Figure S8). The results showed that cell viability was higher than 80% even when the concentration of probe 3 reached 50 μM during the 24 h incubation, indicating that probe 3 has good biocompatibility with live-cell imaging. Confocal microscopy results demonstrated that the HeLa cells treated with probe 3 exhibited strong fluorescence signals, while the presence of H₂S (200 μM) resulted in an obvious fluorescence decrease in the cells. Moreover, an increased H₂S concentration (500 μM) fully abolished the fluorescence signal (Figure S9). In PA cellular imaging experiments, the H₂S-treated group showed a strong PA signal, which was 2.9-fold higher than that of the

control group (only probe 3), implying that probe 3 is capable of detecting H₂S in living cells in a PA turn-on manner (Figure 3). Therefore, probe 3 is suitable for both fluorescence and PA imaging of H₂S in living cells.

Encouraged by the performance of probe 3 in PA cellular imaging, we further explored whether probe 3 can be used for PA imaging of H₂S in a mouse model. We administered two different treatments with the mice: (1) Matrigel was mixed with PBS and then injected into the mice; (2) Matrigel was mixed with H₂S solutions and injected into the mice. After the Matrigel became solid, probe 3 was injected into the solidified sites.⁴⁰ PA images were then acquired every 20 or 35 min. It was noted that PBS with Matrigel showed some background signal (Figure 4), and the signal remained almost unchanged for 75 min after the probe injection. In contrast, in the experimental groups treated with H₂S and probe 3, a 1.8-fold PA enhancement was observed after the probe injection (Figure 4). These results demonstrated that probe 3 is stable in living mice and exhibits a specific PA signal toward H₂S, while the detection depth could reach at least 1 mm. The results indicated that probe 3 has great potential for PA imaging of H₂S in vivo.

CONCLUSIONS

We designed and synthesized a series of dual-modal probes that exhibit interesting controllable H₂S-specific cleavage

activity. The probe produces both PA and fluorescence signal changes when H₂S cleaves the C–N bond in the probe. By tuning of the electron-withdrawing group in the probe, the cleavage rate of the C–N bond could be modulated. Among the different probes, probe 3 showed fast response and good selectivity toward H₂S. Probe 3 was also capable of visualizing cellular H₂S by both fluorescence and PA detection. Furthermore, by taking advantage of PA imaging, probe 3 successfully detected H₂S within 1 mm depth in living mice. Taken together, these results show that this probe can serve as a useful tool for H₂S imaging in living cells and animals by dual fluorescence and PA imaging. The controllable cleavage of the C–N bond reported here will also provide insight for the future development of other new dual-modal H₂S probes. A promising strategy for future study is to conjugate this controllable NBD moiety with a near-infrared dye as a reporter, which would provide a long absorption wavelength for deep-tissue PA imaging. In addition, strong electron-withdrawing groups can be introduced into the probe, and the reaction rate of H₂S-mediated cleavage will be further increased. We envision that our strategy can inspire the development of robust dual-modal probes for biomedical applications.

■ ASSOCIATED CONTENT

Supporting Information

The Supporting Information is available free of charge at <https://pubs.acs.org/doi/10.1021/acsabm.0c00413>.

Synthesis process and NMR and MS characterization of probes 1–3, UV–vis absorption and fluorescence spectra of probe 3 reacted with H₂S, and cell viability and cell fluorescence imaging of probe 3 (PDF)

■ AUTHOR INFORMATION

Corresponding Authors

Hongyan Sun – Department of Chemistry and COSADAF (Centre of Super-Diamond and Advanced Films), City University of Hong Kong, Kowloon, Hong Kong, China; Shenzhen Research Institute of City University of Hong Kong, Shenzhen 518057, China; orcid.org/0000-0003-0932-6405; Email: hongsun@cityu.edu.hk

Lidai Wang – Shenzhen Research Institute of City University of Hong Kong, Shenzhen 518057, China; Department of Biomedical Engineering, City University of Hong Kong, Kowloon, Hong Kong, China; Email: lidawang@cityu.edu.hk

Authors

Jie Zhang – Department of Chemistry and COSADAF (Centre of Super-Diamond and Advanced Films), City University of Hong Kong, Kowloon, Hong Kong, China; Shenzhen Research Institute of City University of Hong Kong, Shenzhen 518057, China

Guohua Wen – Department of Biomedical Engineering, City University of Hong Kong, Kowloon, Hong Kong, China

Wanhe Wang – Department of Chemistry and COSADAF (Centre of Super-Diamond and Advanced Films), City University of Hong Kong, Kowloon, Hong Kong, China; Shenzhen Research Institute of City University of Hong Kong, Shenzhen 518057, China; orcid.org/0000-0002-1458-6263

Ke Cheng – Department of Chemistry and COSADAF (Centre of Super-Diamond and Advanced Films), City University of

Hong Kong, Kowloon, Hong Kong, China; Shenzhen Research Institute of City University of Hong Kong, Shenzhen 518057, China

Qiang Guo – Department of Chemistry and COSADAF (Centre of Super-Diamond and Advanced Films), City University of Hong Kong, Kowloon, Hong Kong, China; Shenzhen Research Institute of City University of Hong Kong, Shenzhen 518057, China

Shuang Tian – Department of Chemistry and COSADAF (Centre of Super-Diamond and Advanced Films), City University of Hong Kong, Kowloon, Hong Kong, China; Shenzhen Research Institute of City University of Hong Kong, Shenzhen 518057, China

Chao Liu – Department of Biomedical Engineering, City University of Hong Kong, Kowloon, Hong Kong, China

Hanrong Hu – Department of Chemistry and COSADAF (Centre of Super-Diamond and Advanced Films), City University of Hong Kong, Kowloon, Hong Kong, China; Shenzhen Research Institute of City University of Hong Kong, Shenzhen 518057, China

Yachao Zhang – Department of Biomedical Engineering, City University of Hong Kong, Kowloon, Hong Kong, China

Huatang Zhang – School of Chemical Engineering and Light Industry, Guangdong University of Technology, Guangzhou, Guangdong 510006, China; orcid.org/0000-0002-9556-2094

Complete contact information is available at:

<https://pubs.acs.org/doi/10.1021/acsabm.0c00413>

Author Contributions

[†]J.Z. and G.W. contributed equally. The manuscript was written through contributions of all authors. All of the authors approved the final version of the manuscript.

Notes

The authors declare no competing financial interest.

■ ACKNOWLEDGMENTS

This work was financially supported by the National Natural Science Foundation of China (21778044, 81627805), the Research Grants Council of Hong Kong (11334516, 11304118, 21205016, 11215817, and 11101618), The Science Technology and Innovation Committee of Shenzhen Municipality (JCYJ20180507181654823 and JCYJ20170413140519030), and the Sichuan Science and Technology Program (2018JY0360).

■ ABBREVIATIONS

H₂S, hydrogen sulfide
PA, photoacoustic
NBD, nitrobenzoxadiazole

■ REFERENCES

- (1) Wang, R. Physiological implications of hydrogen sulfide: a whiff exploration that blossomed. *Physiol. Rev.* **2012**, *92*, 791–896.
- (2) Kabil, O.; Banerjee, R. Enzymology of H₂S biogenesis, decay and signaling. *Antioxid. Redox Signaling* **2014**, *20*, 770–782.
- (3) Kolluru, G. K.; Shen, X.; Bir, S. C.; Kevil, C. G. Hydrogen sulfide chemical biology: pathophysiological roles and detection. *Nitric Oxide* **2013**, *35*, 5–20.
- (4) Tang, G.; Yang, G.; Jiang, B.; Ju, Y.; Wu, L.; Wang, R. H₂S is an endothelium-derived hyperpolarizing factor. *Antioxid. Redox Signaling* **2013**, *19*, 1634–1646.

- (5) Kondo, K.; Bhushan, S.; King, A. L.; Prabhu, S. D.; Hamid, T.; Koenig, S.; Murohara, T.; Predmore, B. L.; Gojon, G., Sr.; Gojon, G., Jr.; et al. H₂S protects against pressure overload-induced heart failure via upregulation of endothelial nitric oxide synthase. *Circulation* **2013**, *127*, 1116–1127.
- (6) Wei, H.-J.; Li, X.; Tang, X.-Q. Therapeutic benefits of H₂S in Alzheimer's disease. *J. Clin. Neurosci.* **2014**, *21*, 1665–1669.
- (7) Paul, B. D.; Sbdio, J. I.; Xu, R.; Vandiver, M. S.; Cha, J. Y.; Snowman, A. M.; Snyder, S. H. Cystathionine γ -lyase deficiency mediates neurodegeneration in Huntington's disease. *Nature* **2014**, *509*, 96–100.
- (8) Hu, L. F.; Lu, M.; Tiong, C. X.; Dawe, G. S.; Hu, G.; Bian, J. S. Neuroprotective effects of hydrogen sulfide on Parkinson's disease rat models. *Aging Cell* **2010**, *9*, 135–146.
- (9) Kamoun, P.; Belardinelli, M.-C.; Chabli, A.; Lallouchi, K.; Chadefaux-Vekemans, B. Endogenous hydrogen sulfide overproduction in Down syndrome. *Am. J. Med. Genet., Part A* **2003**, *116A*, 310–311.
- (10) Wu, D.; Si, W.; Wang, M.; Lv, S.; Ji, A.; Li, Y. Hydrogen sulfide in cancer: friend or foe? *Nitric Oxide* **2015**, *50*, 38–45.
- (11) Lin, V. S.; Chen, W.; Xian, M.; Chang, C. J. Chemical probes for molecular imaging and detection of hydrogen sulfide and reactive sulfur species in biological systems. *Chem. Soc. Rev.* **2015**, *44*, 4596–4618.
- (12) Takano, Y.; Shimamoto, K.; Hanaoka, K. Chemical tools for the study of hydrogen sulfide (H₂S) and sulfane sulfur and their applications to biological studies. *J. Clin. Biochem. Nutr.* **2016**, *58*, 7–15.
- (13) Feng, W.; Dymock, B. W. Fluorescent Probes for H₂S detection and quantification. *Handb. Exp. Pharmacol.* **2015**, *230*, 291–323.
- (14) Yu, F.; Han, X.; Chen, L. Fluorescent probes for hydrogen sulfide detection and bioimaging. *Chem. Commun.* **2014**, *50*, 12234–12249.
- (15) Lippert, A. R. Designing reaction-based fluorescent probes for selective hydrogen sulfide detection. *J. Inorg. Biochem.* **2014**, *133*, 136–142.
- (16) Wang, R.; Dong, K.; Xu, G.; Shi, B.; Zhu, T.; Shi, P.; Guo, Z.; Zhu, W.-H.; Zhao, C. Activatable near-infrared emission-guided on-demand administration of photodynamic anticancer therapy with a theranostic nanoprobe. *Chem. Sci.* **2019**, *10*, 2785–2790.
- (17) Wang, C.; Cheng, X.; Tan, J.; Ding, Z.; Wang, W.; Yuan, D.; Li, G.; Zhang, H.; Zhang, X. Reductive cleavage of C=C bonds as a new strategy for turn-on dual fluorescence in effective sensing of H₂S. *Chem. Sci.* **2018**, *9*, 8369–8374.
- (18) Wang, L. V.; Hu, S. Photoacoustic tomography: in vivo imaging from organelles to organs. *Science* **2012**, *335*, 1458–1462.
- (19) Miao, Q.; Pu, K. Emerging designs of activatable photoacoustic probes for molecular imaging. *Bioconjugate Chem.* **2016**, *27*, 2808–2823.
- (20) Lyu, Y.; Pu, K. Recent advances of activatable molecular probes based on semiconducting polymer nanoparticles in sensing and imaging. *Adv. Sci.* **2017**, *4*, 1600481.
- (21) Ma, T.; Zheng, J.; Zhang, T.; Xing, D. Ratiometric photoacoustic nanoprobe for monitoring and imaging of hydrogen sulfide in vivo. *Nanoscale* **2018**, *10*, 13462–13470.
- (22) Shi, B.; Gu, X.; Fei, Q.; Zhao, C. Photoacoustic probes for real-time tracking of endogenous H₂S in living mice. *Chem. Sci.* **2017**, *8*, 2150–2155.
- (23) Li, X.; Tang, Y.; Li, J.; Hu, X.; Yin, C.; Yang, Z.; Wang, Q.; Wu, Z.; Lu, X.; Wang, W.; et al. A small-molecule probe for ratiometric photoacoustic imaging of hydrogen sulfide in living mice. *Chem. Commun.* **2019**, *55*, 5934–5937.
- (24) Chen, Z.; Mu, X.; Han, Z.; Yang, S.; Zhang, C.; Guo, Z.; Bai, Y.; He, W. An Optical/Photoacoustic Dual-Modality Probe: Ratiometric in/ex Vivo Imaging for Stimulated H₂S Upregulation in Mice. *J. Am. Chem. Soc.* **2019**, *141*, 17973–17977.
- (25) Sun, L.; Wu, Y.; Chen, J.; Zhong, J.; Zeng, F.; Wu, S. A turn-on photoacoustic probe for imaging metformin-induced upregulation of hepatic hydrogen sulfide and subsequent liver injury. *Theranostics* **2019**, *9*, 77.
- (26) An, L.; Wang, X.; Rui, X.; Lin, J.; Yang, H.; Tian, Q.; Tao, C.; Yang, S. The in situ sulfidation of Cu₂O by endogenous H₂S for colon cancer theranostics. *Angew. Chem., Int. Ed.* **2018**, *57*, 15782–15786.
- (27) Wei, C.; Wei, L.; Xi, Z.; Yi, L. A FRET-based fluorescent probe for imaging H₂S in living cells. *Tetrahedron Lett.* **2013**, *54*, 6937–6939.
- (28) Zhang, J.; Wang, R.; Zhu, Z.; Yi, L.; Xi, Z. A FRET-based ratiometric fluorescent probe for visualizing H₂S in lysosomes. *Tetrahedron* **2015**, *71*, 8572–8576.
- (29) Wang, R.; Li, Z.; Zhang, C.; Li, Y.; Xu, G.; Zhang, Q. Z.; Li, L. Y.; Yi, L.; Xi, Z. Fast-Response turn-on fluorescent probes based on thiolysis of NBD amine for H₂S bioimaging. *ChemBioChem* **2016**, *17*, 962–968.
- (30) Huang, Y.; Zhang, C.; Xi, Z.; Yi, L. Synthesis and characterizations of a highly sensitive and selective fluorescent probe for hydrogen sulfide. *Tetrahedron Lett.* **2016**, *57*, 1187–1191.
- (31) Pak, Y. L.; Li, J.; Ko, K. C.; Kim, G.; Lee, J. Y.; Yoon, J. Mitochondria-targeted reaction-based fluorescent probe for hydrogen sulfide. *Anal. Chem.* **2016**, *88*, 5476–5481.
- (32) Zhang, K.; Zhang, J.; Xi, Z.; Li, L.-Y.; Gu, X.; Zhang, Q.-Z.; Yi, L. A new H₂S-specific near-infrared fluorescence-enhanced probe that can visualize the H₂S level in colorectal cancer cells in mice. *Chem. Sci.* **2017**, *8*, 2776–2781.
- (33) Zhang, C.; Zhang, Q.-Z.; Zhang, K.; Li, L.-Y.; Pluth, M. D.; Yi, L.; Xi, Z. Dual-biomarker-triggered fluorescence probes for differentiating cancer cells and revealing synergistic antioxidant effects under oxidative stress. *Chem. Sci.* **2019**, *10*, 1945–1952.
- (34) Yi, L.; Xi, Z. Thiolysis of NBD-based dyes for colorimetric and fluorescence detection of H₂S and biothiols: design and biological applications. *Org. Biomol. Chem.* **2017**, *15*, 3828–3839.
- (35) Song, F.; Li, Z.; Li, J.; Wu, S.; Qiu, X.; Xi, Z.; Yi, L. Investigation of thiolysis of NBD amines for the development of H₂S probes and evaluating the stability of NBD dyes. *Org. Biomol. Chem.* **2016**, *14*, 11117–11124.
- (36) Wang, Y.; Lv, X.; Guo, W. A reaction-based and highly selective fluorescent probe for hydrogen sulfide. *Dyes Pigm.* **2017**, *139*, 482–486.
- (37) Tamura, T.; Song, Z.; Amaike, K.; Lee, S.; Yin, S.; Kiyonaka, S.; Hamachi, I. Affinity-guided oxime chemistry for selective protein acylation in live tissue systems. *J. Am. Chem. Soc.* **2017**, *139*, 14181–14191.
- (38) Tamura, T.; Ueda, T.; Goto, T.; Tsukidate, T.; Shapira, Y.; Nishikawa, Y.; Fujisawa, A.; Hamachi, I. Rapid labelling and covalent inhibition of intracellular native proteins using ligand-directed *N*-acyl-*N*-alkyl sulfonamide. *Nat. Commun.* **2018**, *9*, 1870.
- (39) Montoya, L. A.; Pearce, T. F.; Hansen, R. J.; Zakharov, L. N.; Pluth, M. D. Development of selective colorimetric probes for hydrogen sulfide based on nucleophilic aromatic substitution. *J. Org. Chem.* **2013**, *78*, 6550–6557.
- (40) Sarkar, S.; Ha, Y. S.; Soni, N.; An, G. I.; Lee, W.; Kim, M. H.; Huynh, P. T.; Ahn, H.; Bhatt, N.; Lee, Y. J.; et al. Immobilization of the gas signaling molecule H₂S by radioisotopes: Detection, quantification, and in vivo imaging. *Angew. Chem., Int. Ed.* **2016**, *55*, 9365–9370.